frontiers | Frontiers in Earth Science

TYPE Original Research
PUBLISHED 15 August 2022
DOI 10.3389/feart.2022.967346

OPEN ACCESS

EDITED BY
Wenjun Zheng,
School of Earth Sciences and Engineering, Sun Yat-sen University, China

REVIEWED BY
Huiping Zhang,
Institute of Geology, China Earthquake Administration, China
Weitao Wang,
School of Earth Sciences and Engineering, Sun Yat-sen University, China
Junsheng Nie,
Lanzhou University, China

*CORRESPONDENCE
Junling Pei,
jlpei@qq.com

SPECIALTY SECTION
This article was submitted to Geohazards and Georisks, a section of the journal Frontiers in Earth Science

RECEIVED 12 June 2022
ACCEPTED 05 July 2022
PUBLISHED 15 August 2022

CITATION
Zhou Z, Pei J, Li J, Cai Y and Hou L (2022), High-resolution magnetostratigraphic records of the pliocene sedimentary successions in Yengisar section, NW China, and its tectonic implications.
Front. Earth Sci. 10:967346.
doi: 10.3389/feart.2022.967346

High-resolution magnetostratigraphic records of the pliocene sedimentary successions in Yengisar section, NW China, and its tectonic implications

Zaizheng Zhou[1], Junling Pei[2,3]*, Jianfeng Li[2,3], Yuhang Cai[2,3] and Lifu Hou[2,3]

[1]College of Urban Construction, Heze University, Heze, Shandong, China, [2]Institute of Geomechanics, Chinese Academy of Geological Sciences, Beijing, China, [3]Key Laboratory of Paleomagnetism and Tectonic Reconstruction, Ministry of Natural Resources, Beijing, China

The Neogene strata upward-coarsening sandstone and conglomerate sequences at the periphery of the Northeastern Pamir record the intense uplift of the paleosurface of the building mountains. To further improve our knowledge of source-sink processes, a detailed magnetostratigraphic investigation was carried out along the Yengisar section, which is located at the southwestern margin of the Tarim Basin. The new high-resolution magnetostratigraphic data revealed that the Artux Formation was deposited from 4.9 Ma to 1.9 Ma with three sedimentation rates changes. The variations in sedimentation rate may be due to the pulsating exhumation of the Western Kunlun Mountain, caused by the northward motion of the Pamir salient. By integrating the evidences from the seismic reflection profile and other magnetostratigraphic investigations in this region, the basal age of the Xiyu Formation and the early stages of growth strata deposition were estimated at ~1.9 and 1.45 Ma, respectively. Based on the data, we propose that the progradation of the Xiyu Formation and the migration of the deformation front are the two independent responses of the sink region to the uplift events of the source region.

KEYWORDS

magnetostratigraphy, Pliocene, Pamir salient, sedimentation rate, Southwestern Tarim

Introduction

The Indo-Eurasia continental collision resulted in the deformation of the Western syntax of the Tibetan Plateau (Pamir Plateau), which is considered as one of the most remarkable regions in the globe (Burtman and Molnar, 1993; Zhao et al., 2008a; Cowgill, 2010; Chen et al., 2014) (Figure 1). In fact, the collision is responsible for the formation of the Paratethys Sea, the northern branch of the Neo-Tethys Ocean, which retreated to the Mediterranean during the Cenozoic (Bosboom et al., 2011; Sun and Jiang, 2013; Bosboom et al., 2014; Sun et al., 2016; Li et al., 2017). Furthermore, the Cenozoic tectonic processes have shaped the present surface topography, which is considered as a gigantic orogeny-basin coupling system (Kunlun Mountain, Tian Shan, and Tarim Basin) (Cao et al., 2018; Li et al., 2019). The Tarim Basin preverves more than 10 km thick of Cenozoic strata, which provide an excellent chance to testif the tectonic evolution of the plateau uplift based on high-resolution age constrains. Thus, dating the depositional age of the Cenozoic sedimentary successions is crucial to understanding the coupling mechanism between the mountain building, sediment deposition, and aridification history.

In the Southwestern Tarim Basin, substantial sections containing the Cenozoic strata at the piedmont of the Tian Shan and the Kunlun Mountain are incised by the drainage system shed from the growing plateaus or highlands (Figures 1, 2A). In recent years, considerable attention has been devoted to these well-exposed outcrops to decipher the paleogeographic evolution (e.g. Zheng et al., 2000; Chen et al., 2002; Chen et al., 2007a; Chen et al. 2007b; Huang et al., 2006; Charreau et al., 2006; Heermance et al., 2007; Pei et al., 2008; Pei et al., 2011a; Pei et al., 2011b; Bosboom et al., 2011; Bosboom et al., 2014; Sun and Jiang, 2013; Tang et al., 2015; Yang et al., 2015; Chen et al., 2015; Qiao et al., 2016; Qiao et al., 2017; Zhou et al., 2016; Liu et al., 2017). Magnetostratigraphy is the most widely applied and most powerful method, due to a lack of diagnostic fossil and volcanic layers in continental deposits. Previous studies have focused mainly on the following three important scientific problems: 1) When did the Para-Tethys Sea finially retreat from the Tarim Basin (Guo et al., 2002; Bosboom et al., 2011; Bosboom et al., 2014; Sun and Jiang, 2013; Sun and Jiang, 2016; Yang et al., 2015; Zhang et al., 2001); 2) How did the accumulation of the Tarim Basin response to the global climate changes (Sun and Liu., 2006; Charreau et al., 2009; Pei et al., 2011a; Zheng et al., 2015a); 3) the uplift processes of the Western tectonic syntax and the Tian Shan (Zheng et al., 2000; Chen et al., 2002; Huang et al., 2006; Pei et al., 2011b; Chen et al., 2015; Qiao et al., 2016). The stratigraphic attribute and the origin of the Late Cenozoic deposits consisting of the Artux Formation and the Xiyu Formation (Xiyu Conglomerate) had been widely studied in the past decades. Most researchers have considered that the upward-coarsening sediments recorded an abrupt change in paleoslope, as a result of immense surface uplift in the mountains (Huang 1957; Li et al., 1979; Zheng et al., 2000), while others believe it was triggered by dramatic climate changes at ~2–4 Ma ago (Molnar et al., 1993; Zhang et al., 2001; Wang et al., 2003; Charreau et al., 2009).

To better decipher the spatial characteristics and deformation behavior of the uplift-related molasse deposits, here we conduct a new magnetostratigraphic study in detail in the Yengisar section located at the southwestern margin of the Tarim Basin. Moreover, we discussed the sedimentation rate changes of the Pliocene secessions and their potential causes. Combining with other magnetostratigraphic data and

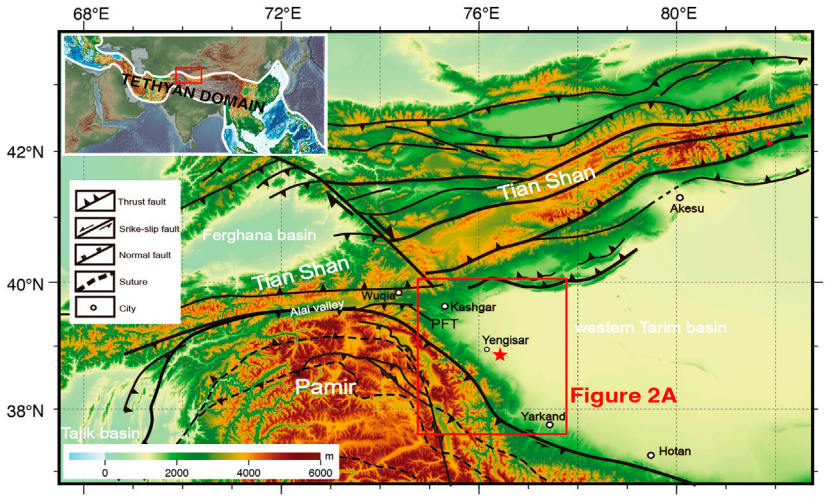

FIGURE 1
Simplified tectonic map of the western Tarim Basin and its surrounding orogens (after Xu et al., 2011; Li et al., 2017).

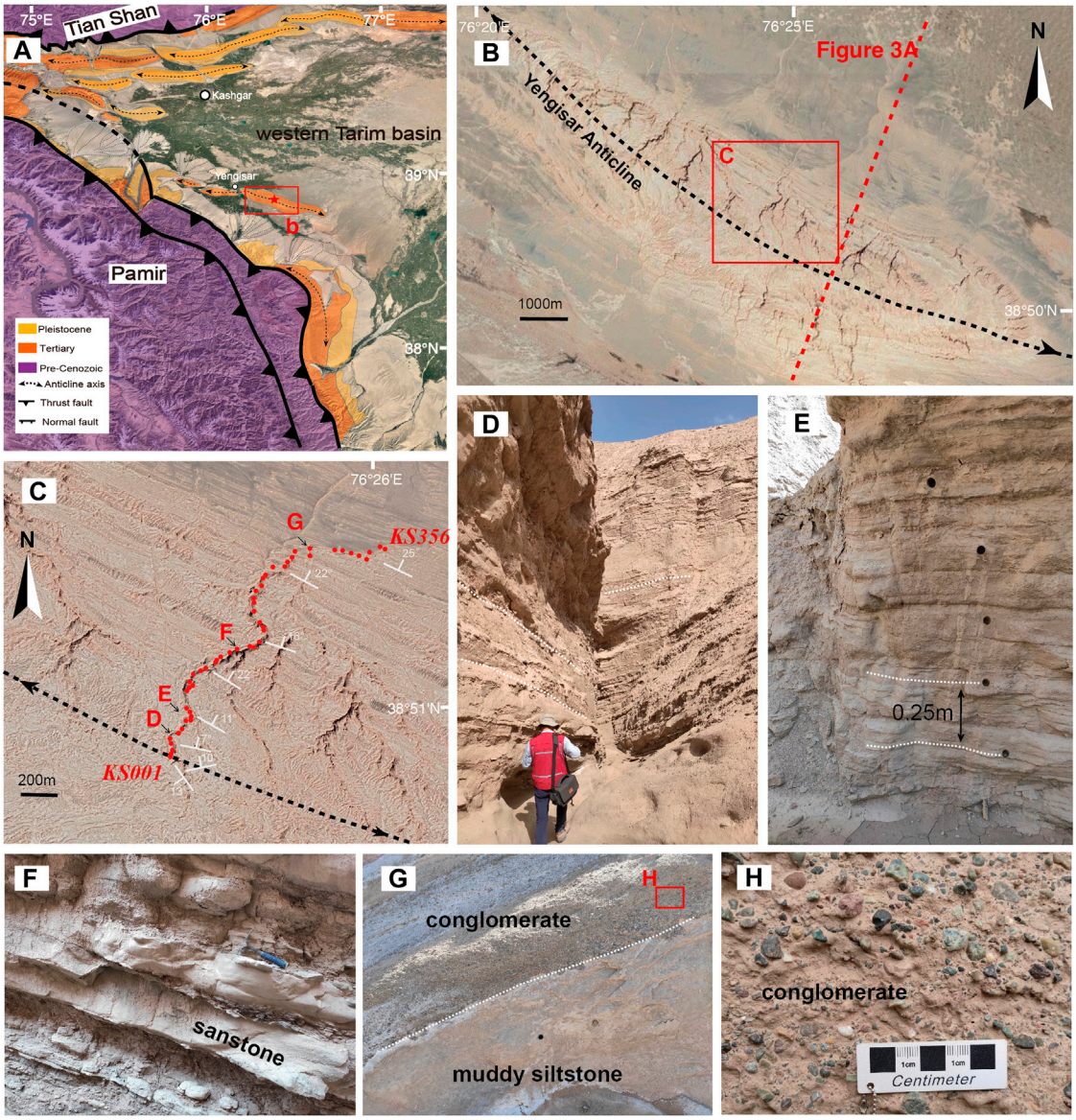

FIGURE 2
(A) Geological sketch map of the study area with highlighting on the Cenozoic strata distribution (after Pan et al., 2009). The red aster denotes the location of the studied section. **(B)** and **(C)** show the detailed sampling sites along the canyon across the northeast limb of the Yengisar anticline. **(D)**, **(E)**, **(F)**, **(G)**, and **(H)** show the stratigraphy, lithology and sampling snapshot in the fieldwork, the spots for photography are marked in **(C)**.

geophysical evidence, we further summarized the attribution of the variational basal age of the Xiyu Formation.

Regional geological setting and stratigraphy

The Western Tarim Basin is a depression surrounded by the Tian Shan to the north and the West Kunlun Mountain to the southwest. The long and the short distance effects of the Indo-Eurasia collision during the Cenozoic caused a strong uplift, shortening, and strike-slip deformation in the surrounding areas of the Western Tarim Basin (Figures 1, 2A) (Xu et al., 2011; Chen et al., 2014). As part of the large-scale Meso-Cenozoic sedimentary basin in the West of China, the Western Tarim Basin preserves over 10 km thick strata, which becomes thinner in the east (Chen et al., 2001; Li et al., 2019).

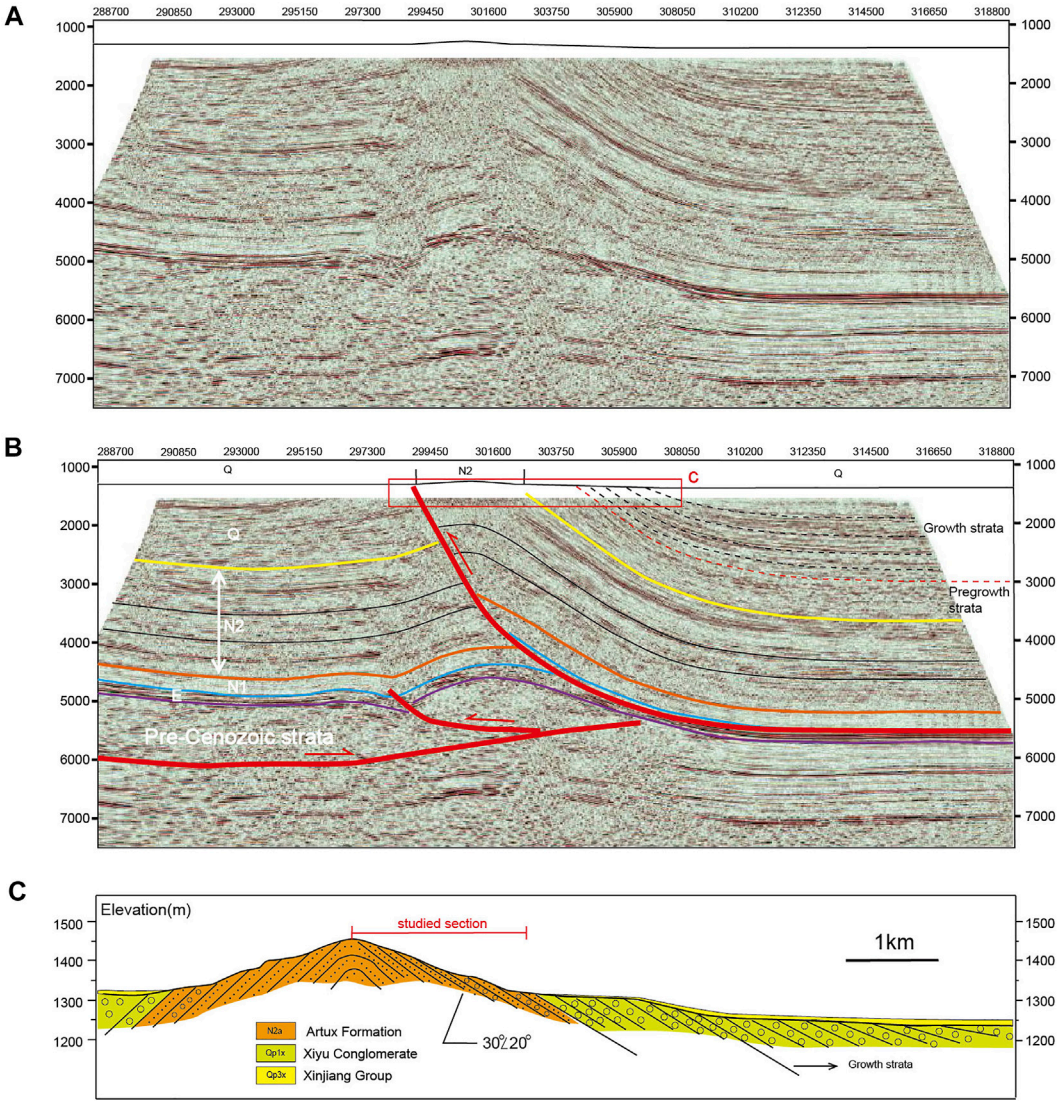

FIGURE 3
(A) and **(B)**, Seismic reflection profile and its interpretation (by Gao, 2012). The location of the survey line was displayed in Figure 2B. The profile shows that the boundary (yellow solid line) between the Artux Formation and the Xiyu Conglomerate is near the top of the studied successions. The basal layer (red dot line) of the growth strata (black dot lines) is deposited within the Xiyu Conglomerate. **(C)**, The schematic diagram for the sampling section as demonstrated in **(B)**.

The lithostratigraphy of the Cenozoic sequences in the Western Tarim Basin along the western Kunlun-Pamir was divided into the Paleogene Kashi, the Miocene Wuqia groups, the Artux Formation, and the Xiyu Formation. Indeed, the Kashi Group is composed of the Aertashi, Qimugen, Gaijitage, Kalatar, Wulagen, and Bashibulake formations in ascending order, recording series of marine transgressions and regressions, while the Wuqia group, including the Keziluoyi, Anjuan, and Pakabulake formations, was deposited in a terrestrial environment (BGMRXJ, 1999; Guo et al., 2002; Bosboom et al., 2014; Chen et al., 2015; Sun et al., 2016; Li et al., 2017; Zhang et al., 2001).

In this study, we focused on the Artux Formation in the Yengisar section during the Pliocene epoch (Figure 2A). The Artux Formation consists of fluvial, yellow-gray to tan mudstone, siltstone, and fine- to medium-grained sandstone which generally coarsen upward (Zheng et al., 2002; Pei et al., 2008). The lithology of the upper part of the Artux Formation is marked by an abrupt coarsening and darkening (Figure 2). On the other hand, the Xiyu Formation overlies conformably the Artux Formation and is dominated by massive, thickly bedded, and

pebble-to-cobble conglomerates, typical of the channel and debris-flow deposits of alluvial fans and gravel-bed braided rivers, locally interbedded with minor lenticular sandstone and mudstone beds in its lower part (Chen et al., 2000; Chen et al., 2007a; Zhang et al., 2001).

Materials and methods

The sampled section is exposed in an eroded canyon. It is located in the middle of the northeast flank of the Yengisar anticline, about 25 km southeast of the Yengisar county (Figure 2). In the Yengisar, the strike fold anticline axis is N20°W. In fact, the sampled section is almost perpendicular to the fold axis, with a horizontal width of about 2 km (Figures 2B,C). The dipping strata direction is Northeast, with an angle ranging from 10° to 25°. According to the field measurement result in this study, the true thickness of the section is about 520 m. In addition, based on the abutting seismic profile of the section (Gao, 2012), the upper part of the Artux Formation is exposed in the canyon (Figures 2, 3), because it was covered by the diluvial fan sediments of the Xinjiang Group during the late Quaternary. Nevertheless, no contact between the Artux Formation and the Xiyu Formation at the top of the section was observed. The transitional contact should be near the top of the sampled section, to identify the basal layer of the growth strata developed in the Xiyu Formation (Figure 3B).

In total, 356 oriented core samples were collected from the bottom to the top of the sedimentary sequence using a portable gasoline-powered drill (Figures 2C, 3C), at a sampling interval of 0.25 m (if the petrology is available) (Figure 2E). Indeed, an interval of multiple meters was considered where the sequence is composed mostly of coarse sandstone and granule conglomerate (Figures 2G,H; Supplementary Figure S1). All the core samples were oriented first by magnetic compass after a local declination correction, determined from the International Geomagnetic Reference Field (IGRF), and then cut into cylindrical specimens using a double-bladed saw in the laboratory.

The rock magnetic experiments for representative specimens were conducted at the Key Laboratory of Paleomagnetism and Tectonic Reconstruction of the Ministry of Natural Resources, Institute of Geomechanics, Beijing. The temperature-dependence of magnetic susceptibility (κ-T curve) was carried out using the Kappabridge KLY-4, equipped with a CS-4 high-temperature furnace (Agico Ltd., Brno), by heating from room temperature to 700°C, followed by cooling back to room temperature. In addition, the first-order reversal curves (FORCs) and magnetic hysteresis loop were obtained using a Princeton Vibrating Sample Magnetometer (MicroMag 8600 VSM). The FORCs diagrams were illustrated by FORCinel (v 3.06) using a smoothing factor value of 3 (Harrison et al., 2018).

In total, 331 specimens collected from the Yengisar section were subjected to stepwise thermal demagnetization (TD) experiment using a thermal demagnetizer (TD-48) in a magnetically shielded room, with a residual magnetic field of less than 300 nT. After each step of TD, remanent magnetizations were measured using a 2G-755 cryogenic magnetometer at the Key Laboratory of Paleomagnetism and Tectonic Reconstruction of the Ministry of Natural Resources, Institute of Geomechanics, Beijing. For all specimen, the demagnetization was carried out first within a temperature interval of 40°C or 100°C to 500°C, and subsequently in steps of 20°C or 10°C to 680°C.

The demagnetization results were analyzed using principal component analysis (PCA) (Kirschvink, 1980) and Fisher statistic methods (Fisher, 1953). Furthermore, paleomagnetic data were analyzed using the online software paleomagnetism.org (Koymans et al., 2020).

The anisotropy of magnetic susceptibility (AMS) of 326 specimens was measured using the KLY-4 Kappabridge susceptibility meter at the Key Laboratory of Paleomagnetism and Tectonic Reconstruction of the Ministry of Natural Resources, Institute of Geomechanics, Beijing.

Results

Rock magnetic experimental results

Two representative samples were selected from the section for rock magnetic experiments, to obtain the behavior of magnetic materials. As shown in the κ -T curve diagrams (Figures 4A,B,E,F), the heating curves of the KS78 and KS297 have gradually decayed to 680°C, indicating that hematite is the dominant magnetic carriers in the collected samples. However, the cooling curves were remarkably higher than the heating curves, due to the formation of new magnetic minerals during the heating process. The magnetic hysteresis loop revealed that the representative samples are fully saturated at an applied field of 2 T, with a low coercivity of about 10–15 mT (Figures 4C,G). The shape of hysteresis loop show that samples have obvious characteristics of wasp-waisted, which may indicate that the magnetic minerals in the sediments are mainly the mixture of single-domain (SD) and superparamagnetic (SP) particle sizes or the combination of different kinds of magnetic minerals (Tauxe et al., 1996). Moreover, the FORC diagrams obtained show that samples were dominated by SD and pseudo-single domain (PSD) particles (Figures 4D,H). Rock magnetic results suggest that SD hematite is the primary magnetic carrier mineral in the sedimentary rocks of the Yengisar section.

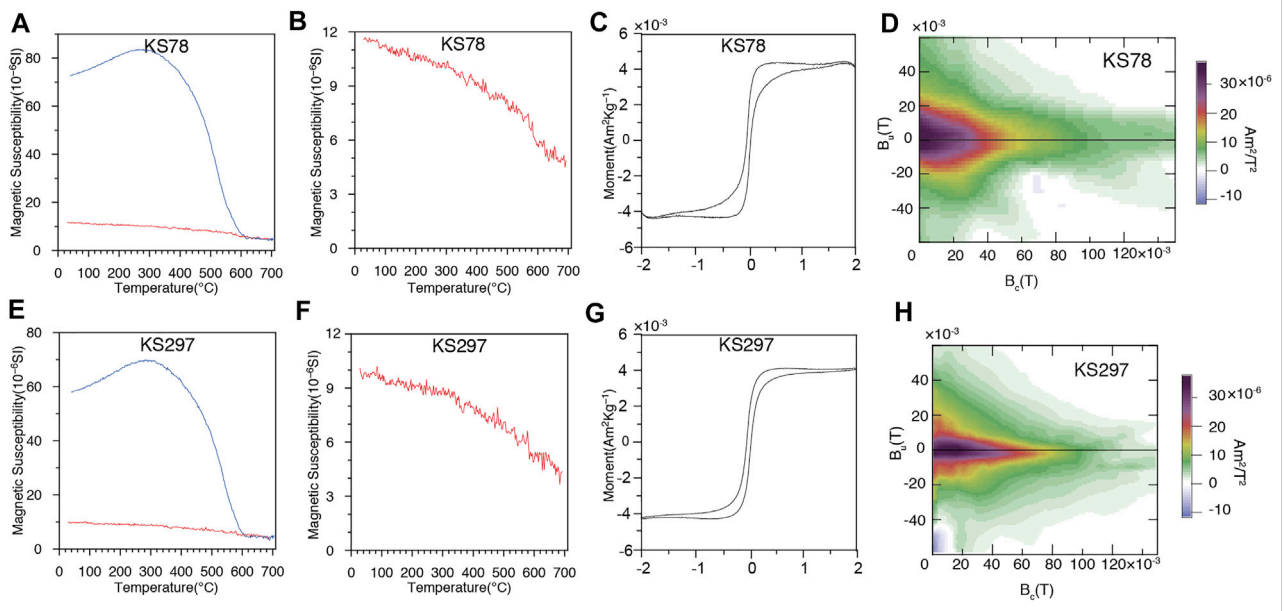

FIGURE 4
Rock magnetism for representative specimens. **(A)**, **(B)**, **(E)**, and **(F)**, thermomagnetic susceptibility curves. **(C)** and **(G)**, magnetic hysteresis loops. **(D)** and **(H)**, first-order reversal curves (FORCs).

Demagnetization

After the removal of viscous remanent magnetization at a temperature generally below 200°C, one stable magnetization component was extracted from the 322 samples collected from the upper part of the Artux Formation. Demagnetization behaviors of the remanent magnetization showed a linear decay to the origin at about 680°C (Figure 5). Indeed, nine specimens showed noisy thermal demagnetization behaviors, making isolation of the characteristic remanent magnetization (ChRM) difficult (Figure 5D). On the other hand, 322 ChRMs were of dual polarity and have passed the reversal test (Figures 6A,B). All the negative ChRMs are flipped to positive. Then 48 ChRM directions was rejected after a 45-cutoff and the remains reported a mean direction value of $D_g = 330.6°$, $I_g = 61.1°$ ($k = 17.6$ $\alpha_{95} = 2.2°$) before and $D_s = 355°$, $I_s = 46.6°$ ($k = 16.6$, $\alpha_{95} = 2.1°$) after tilt correction (Figures 6C–F).

Magnetostratigraphy

To define magnetic polarity zones (Figure 7), all the ChRM directions were used to calculate the virtual geomagnetic pole (VGP) and were plotted against stratigraphic levels.

The obtained result showed four pairs of normal and reverse polarity zones (N1-N4, R1-R4) with four tentative narrow intervals (inferred by less than three continuous specimens) (Figure 7). Based on the seismic reflection profile, it is inferred that about 2 km thick of Artux Formation below the Xiyu Formation was developed in this region, while the studied section contains 520 m thick strata of the upper part of the formation, which have continuous contact with the overlying layers (Figure 3).

According to several authors, the basal age of the Artux Formation and the upper limit age are time-transgressive (Zheng et al., 2000; Chen et al., 2002; Chen et al., 2007b; Heermance et al., 2007; Chen et al., 2015; Qiao et al., 2016; Qiao et al., 2017). Furthermore, the chronology of the sedimentary package in the same section remains different. Zheng et al. (2000) reported that the Artux Formation, exposed in the Kekeya section at the southwestern edge of the Tarim Basin, is dominated by a long-reversed polarity zone, and assumed to correlate with the Gibert reversed chron. Thus, the Artux Formation has a depositional age ranging from 4.6 to 3.5 Ma (Figure 2A). Volcanic tuff intercalated in the Xiyu Formation was recently identified in the Kekeya section. Based on new radioisotopic data, the stratigraphic age of the Artux Formation ranges from ~22.6 to 15 Ma (Zheng et al., 2015a; Zheng et al., 2015b; Sun et al., 2015). Since the depositional onset of this coarse clastic episode is diachronous, the Artux Formation was considered as a lithostratigraphic unit, rather than a chronostratigraphic marker (BGMRXJ, 1999). Based on the traditional opinion adopted, the Artux Formation is believed to be deposited approximately during the Pliocene, rather than the early Miocene, due to the micropaleontologic

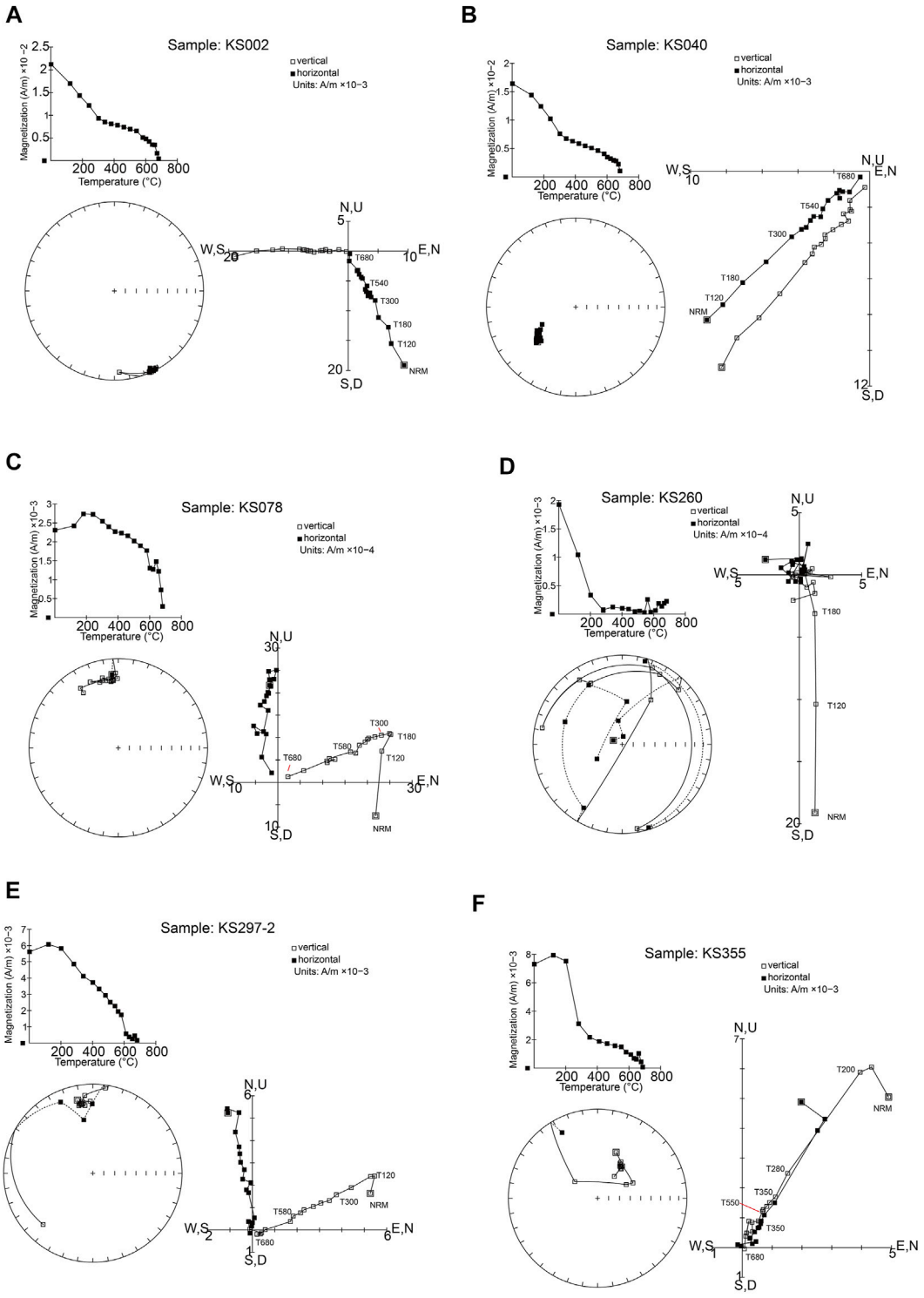

FIGURE 5
Zijderveld vector diagrams and Equal-area plots for representative specimens. **(A)** Sample: KS002, **(B)** Sample: KS040, **(C)** Sample: KS078, **(D)** Sample: KS260, **(E)** Sample: KS297-2, **(F)** Sample: KS355.

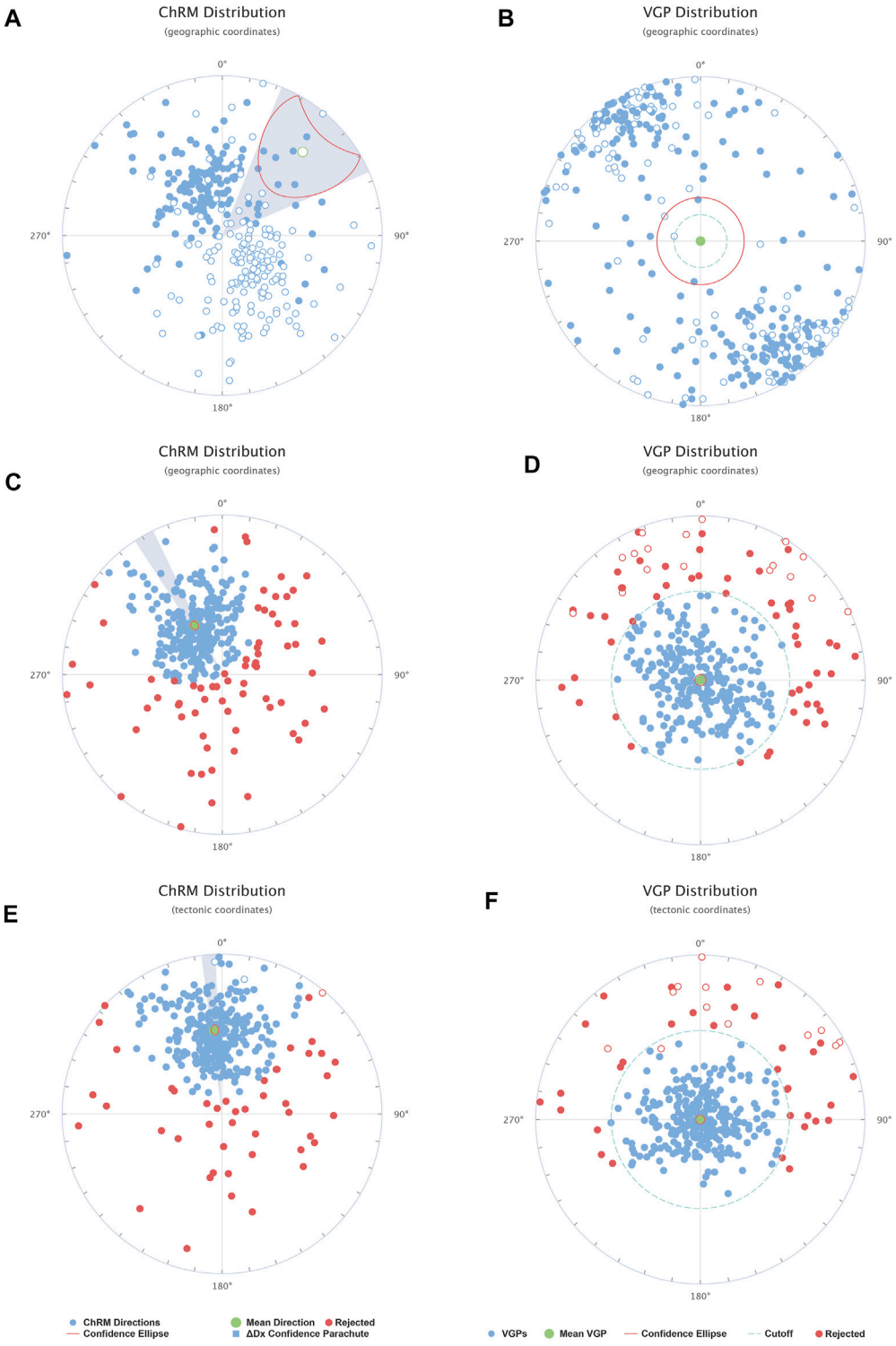

FIGURE 6
In-situ [geographic coordinates, **(A, B, C, D)**] and tilt-corrected [tectonic coordinates, **(E, F)**] Equal-area stereographic projection of ChRMs and VGPs from the Yengisar section. **(A)** and **(B)** show the raw data of dual polarity. **(C)**, **(D)**, **(E)** and **(F)** show the pattern after 45-cutoff of all ChRMs contain positive and flipped directions.

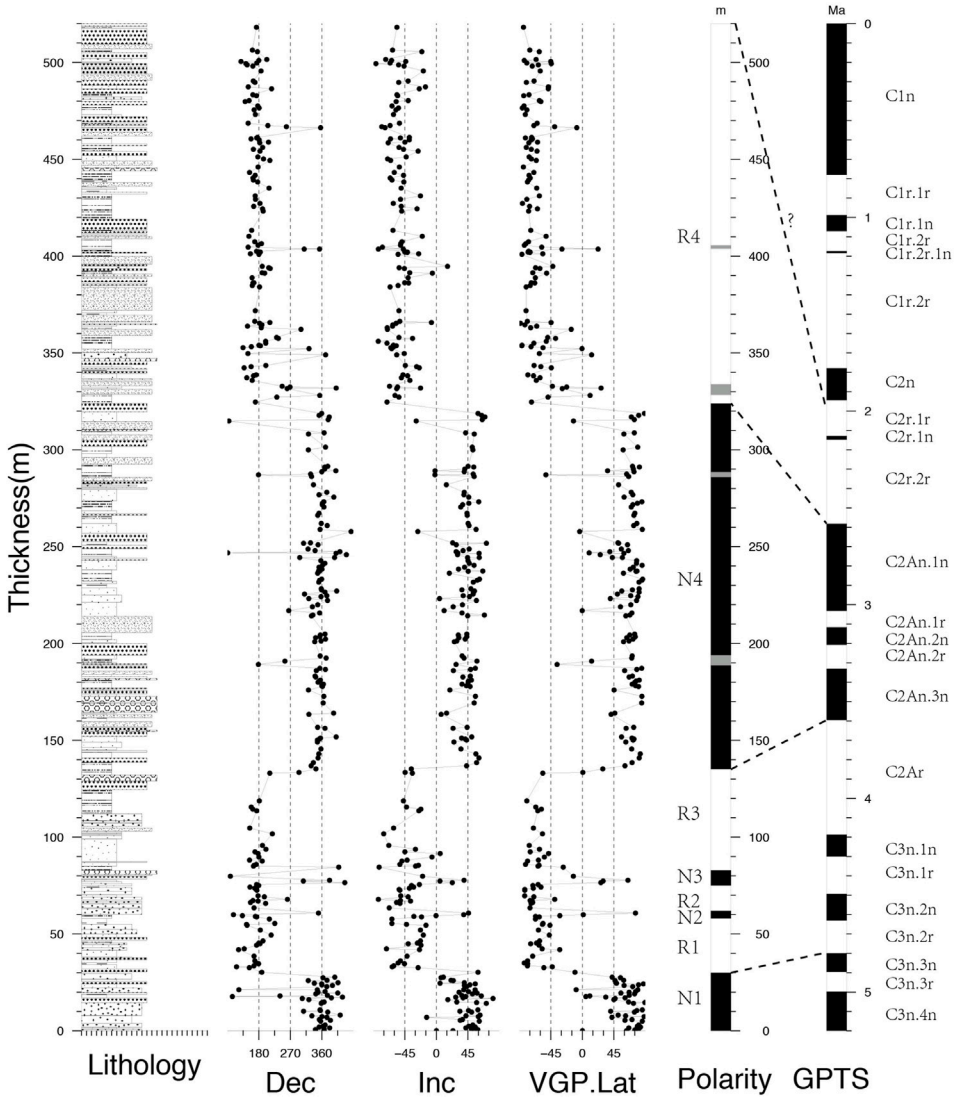

FIGURE 7
Lithology and magnetostratigraphic results from the Yengisar section in the western Tarim Basin. The characteristic remanence declination and inclination and VGP latitude are plotted as a function of stratigraphic level and the correlation with the geomagnetic polarity time scale (Gradstein et al., 2012).

evidence. Indeed, this formation contained Ostracoda and Charophyta assemblages, of which *Eucypris notabilis, Advenocypris decuria, and Candona neglecta* were found in the Pliocene strata in Russian, while *Cyprideis punctillata* was observed in the Pliocene strata series in the Qaidam basin (BGMRXJ, 1999). The micropaleontologic evidence for regional correlation with sedimentary sequence indicated that the lithostratigraphic ages of the Artux Formation cannot be much older than 5.3 Ma.

With these constraints, the magnetostratigraphy for the terrestrial sequence of the studied section can be reconstructed. The complete pattern of magnetic polarity zones presented in Figure 7, was correlated with the GPTS 2012 (Gradstein et al., 2012). In fact, the middle part of the polarity zones (N4) can be correlated to C2An. Moreover, the magnetic polarity zones from N1 to R3 were correlated with chrons C3n2r through C2Ar. While the long-reversed intervals R4 were correlated to C2r.

According to the correlation analysis, the depositional age of the contiguous sedimentary package in the Yengisar anticline section varies from 4.9 to 1.9 Ma.

Anisotropy of magnetic susceptibility

The AMS can measure the rock fabrics, potentially governed by depositional conditions or post-depositional sedimentary

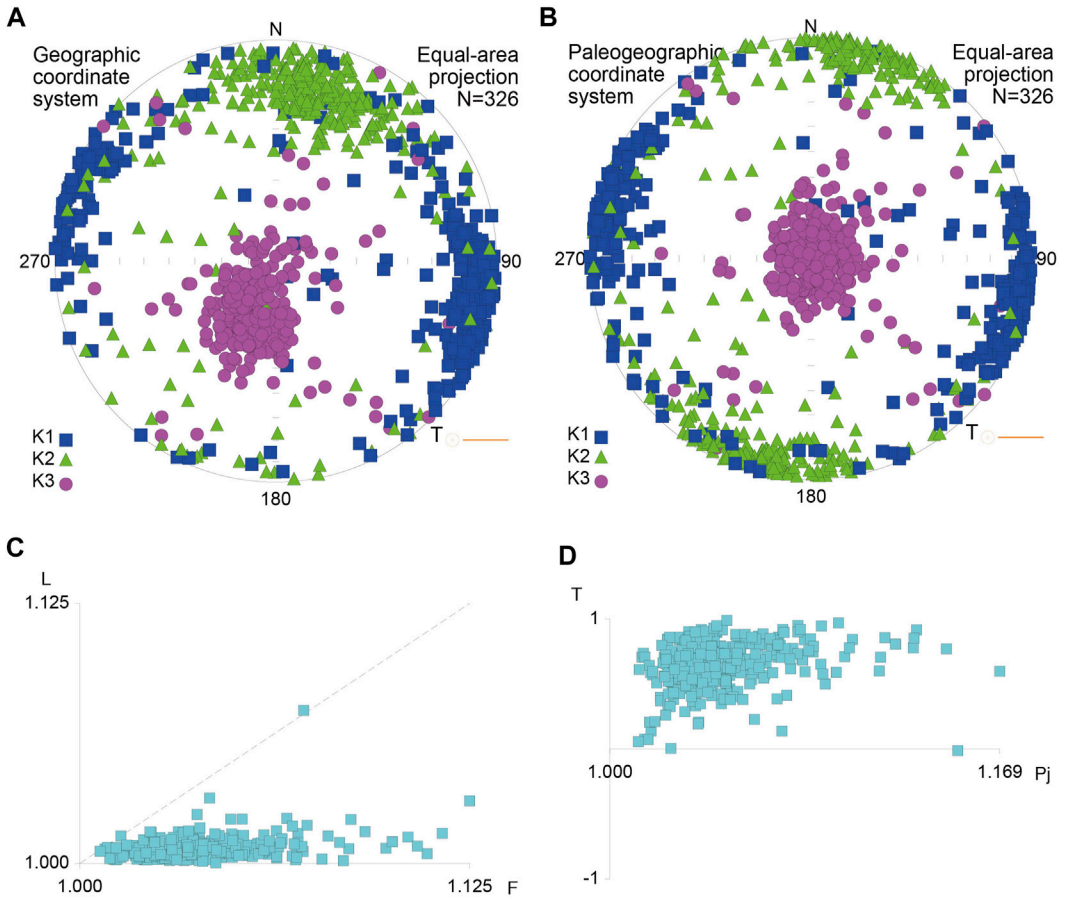

FIGURE 8
Anisotropy of magnetic susceptibility (AMS) results from the Yengisar section. Stereographic projections (lower hemispheres) of AMS orientations before **(A)** and after **(B)** tilt correction. **(C)**, F (foliation)-L (lineation) diagram. **(D)**, P_j–T (corrected AMS degree versus AMS shape parameter) plot.

process. This technique can also record the imprint of later tectonism (Borradaile and Henry, 1997; Borradaile and Jackson, 2004).

The AMS ellipsoids of the Artux Formation from the Yengisar anticline are typical primary sedimentary fabrics (Figure 8). This kind of magnetic fabric is controlled by depositional and diagenetic processes and is characterized by oblate AMS ellipsoids with maximum and intermediate susceptibility axes (K_1 and K_2, respectively) within the bedding plane, and minimum susceptibility axis (K_3) perpendicular to the bedding plane (Figure 8B). All specimens plot in the oblate region ($K_1 \approx K_2 > K_3$) on F (foliation)-L (lineation) and P_j (corrected anisotropy)-T (shape parameter) diagram (Figures 8C,D).

The AMS parameters were filtered individually, and weights were given based on Gaussian function, with 20 m intervals in stratigraphic levels (Figure 9). The filtered data identified the trend of signal changes. As seen in Figure 9, the bulk magnetic susceptibility (K_m) values range from 200 to 400 μSI, with a gradual decrease from the base level of this section (0 m, ~4.6 Ma) to the middle layers at 250 m (~2.9 Ma). After an abrupt increase in the K_m value, a second gradual decreasing trend to the 430 m level (~2.1 Ma) was observed (Figure 9). The overall low values of bulk susceptibility indicate that paramagnetic and antiferromagnetic minerals such as clays and hematite, predominantly control both the susceptibility and anisotropy of these studied sediments (Tarling and Hrouda, 1993), which is consistent with the rock magnetic results.

The P_j values range from 1.012 to 1.169, with a mean of 1.049. Indeed, the low P_j values and the relatively constant high level of spherical shapes (T) indicate that the magnetic anisotropy is the result of the compaction effect. The corrected anisotropy (P_j) values showed a similar trend as compared to the K_m parameter (Figure 9), resulting in a weak positive correlation ($r = 0.43$). On the other hand, a weak negative correlation ($r = -0.33$) was observed between the spherical shapes and the declinations of K_1 (Figure 9). This finding can be explained by the fact that the

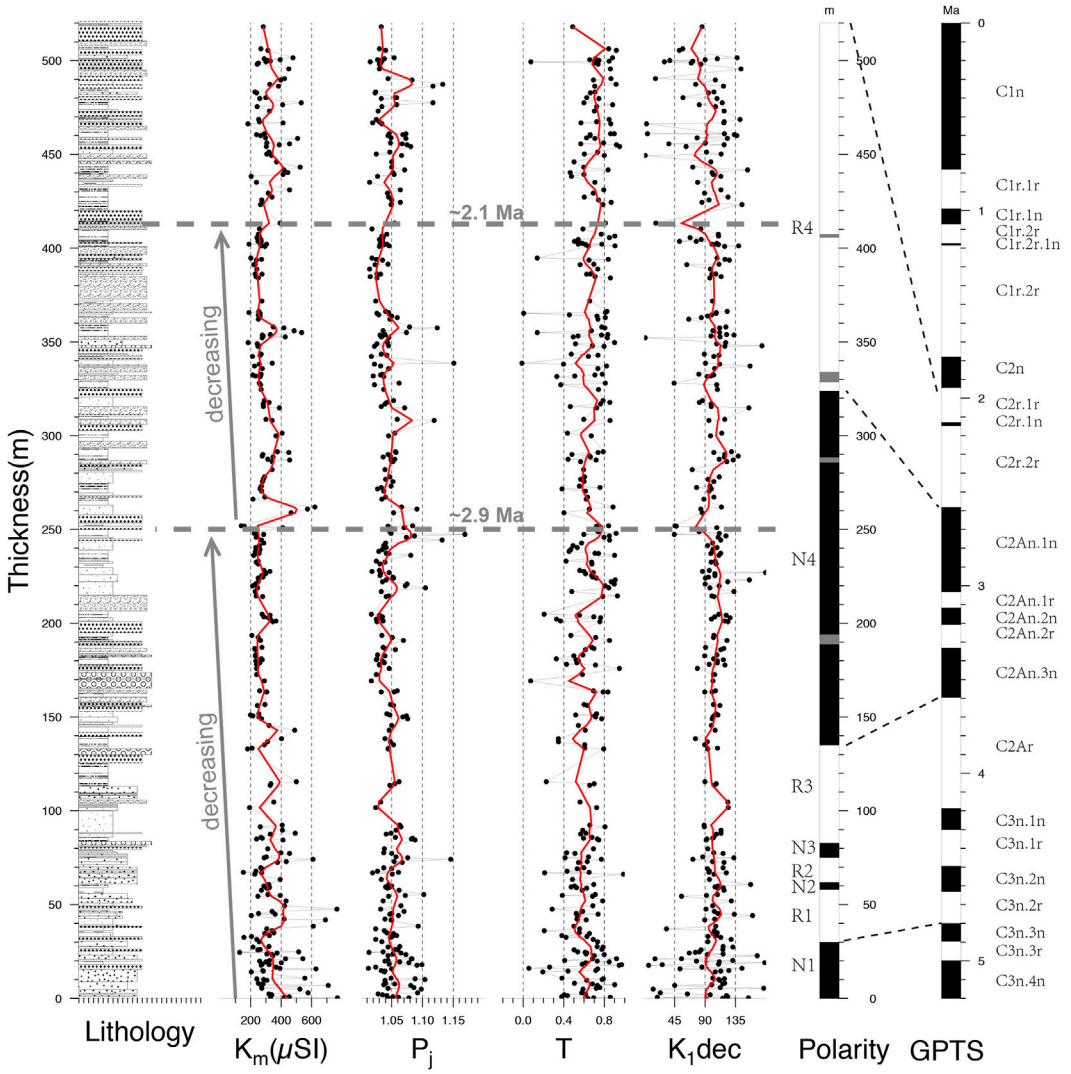

FIGURE 9
Magnetic susceptibility (K_m), the Degree of Anisotropy (P_j), the Shape Parameter (T) and the direction of the maximum susceptibility axes (K_1) as a function of depth in the Yengisar section. The red curves are obtained by data filtering, weights are given by Gaussian function with 20 m intervals in stratigraphic levels.

shapes of the AMS ellipsoids are generally influenced by the combination of depositional compaction and paleocurrent or compresisional stress field.

Discussion

Changes in sedimentation rate and its triggers

The sedimentation rate can be determined by magnetostratigraphic ages and stratigraphic thicknesses (Figure 10A). The results revealed that the sedimentary rates were not corrected for post-depositional compaction, due to the unknown history of compaction. In addition, the Tarim Basin is internally filled, and the total sediment flux directly reflects the denudation rates over the source region. Therefore, rates represented here should be minima that show how sedimentation rate change at specific localities relative to the topographic evolution of the range (Metivier and Gaudemer, 1997; Charreau et al., 2006). As reported above, the directions of the paleo-drainages were E-W to SEE-NWW, as indicated by the K_1 directions (Figure 9). In addition, the Pliocene alluvial occurs mostly at the outlets of modern rivers, were responsible for the Artux Formation (Figure 11). These two pieces of evidence indicate that the

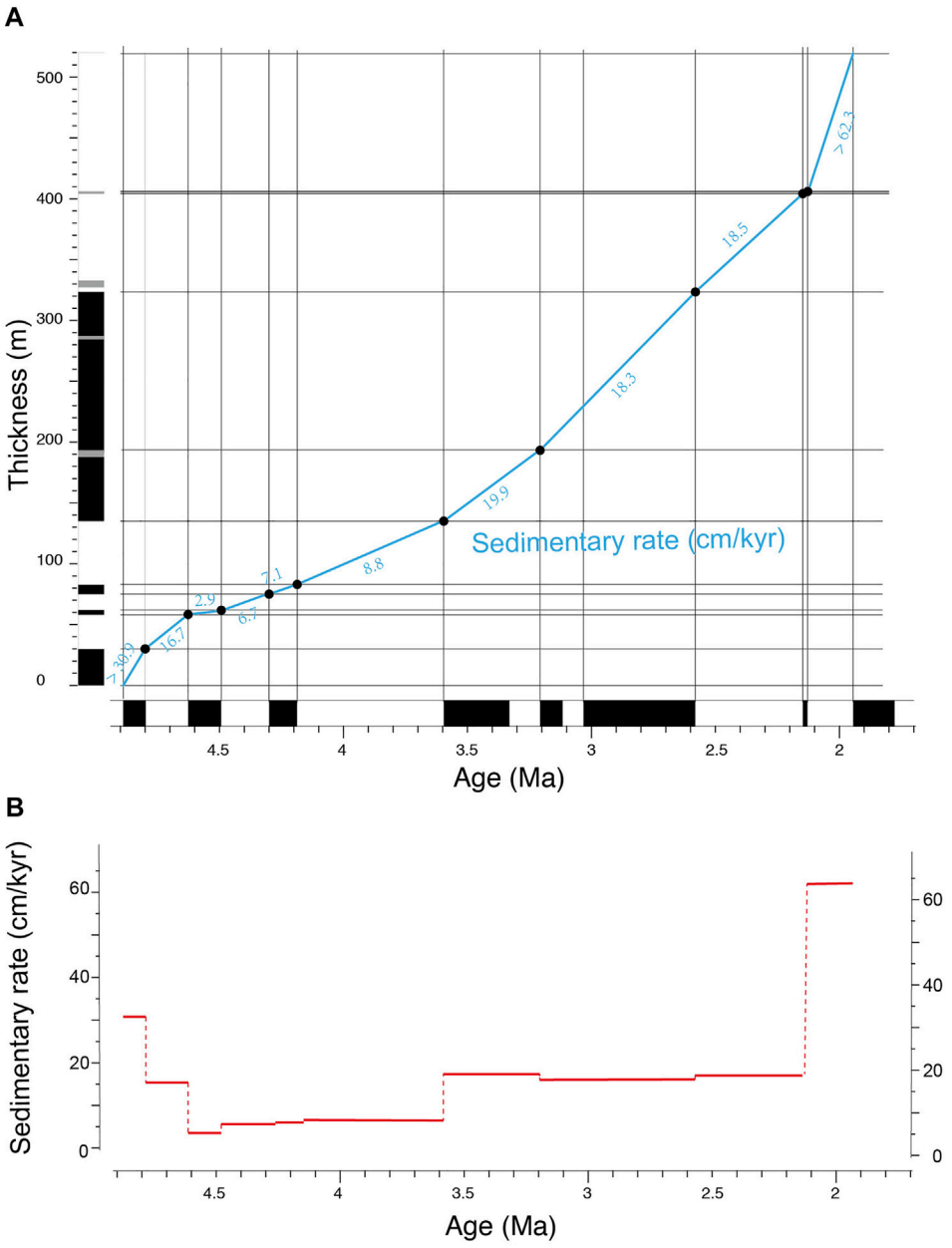

FIGURE 10
The stratigraphic height as a function of magnetostratigraphic age in the Yengisar succession of the western Tarim Basin showing sedimentation rates in the studied section. **(A)** Plot of the sedimentary thickness versus time; **(B)** Plot of sedimentary rate variation over time.

provenance of the Pliocene sedimentary secessions in Yengisar anticline is the West Kunlun Mountain rather than the South Tian Shan.

The magnetostratigraphic age plot within the composite section (Figure 10A) showed a gradual decrease in sedimentation rate, from >30.9 cm/kyr to 2.9 cm/kyr during the 4.9–4.6 Ma period, representing about 10-fold change. This may be due to the presence of weakened topographic uplift in the provenances and the subsequent equilibrium patterns between erosion and deposition in the same regions. The sedimentation rate period (2.9 cm/kyr) continues about 0.1 Myr (Figure 10A). Abrupt increases in sedimentation rate ranging from ~8 cm/kyr to ~19 cm/kyr and from ~19 cm/kyr to >62.3 cm/kyr were observed at 3.6 Ma and 2.1 Ma, respectively. By

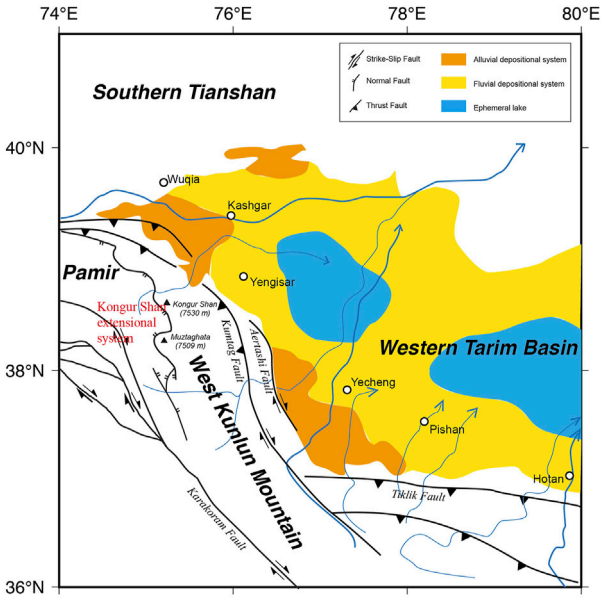

FIGURE 11
Tectonic outline and depositional systems of the Western Tarim Basin and its surroundings during the Pliocene (Robinson et al., 2004; Wei et al., 2013).

considering the ascending order of the frequent and thicker massive coarse sandstone layers, it is argued that these two changes in sedimentation rate explain the move away from the denudation region, which was more likely induced by the strong basinward thrusting of the orogenic belts adjacent to the western Tarim Basin that has occurred since the Pliocene (Qu et al., 2004; Wei et al., 2013).

The first decrease (at ~4.6 Ma) and the two subsequent increases (at 3.6 Ma and 2.1 Ma) in the sedimentation rate indicate that the Western Kunlun Mountain was characterized by pulse and strength uplift events during the Pliocene epoch (Figure 10B).

However, distinguishing between tectonic and climatic forces on sedimentation rate changes is not straightforward (Molnar and England, 1990). According to Zhang et al. (2001) and Wang et al. (2003), the significant increases in grain sizes of sediments and sedimentation rate were governed by climate changes during the Pliocene period. Based on the tectonically driven hypothesis, the tectonic uplift events were among the first-order control factors. An abrupt and frequent climate change since ~5 Ma was considered responsible for the disequilibration of the landscape's erosion (Zhang et al., 2001; Westerhold et al., 2020). If the denudation region was in a weaken uplift activity a new equilibrium configuration is expected to be reestablished after a higher sedimentation time. Since the Pliocene, the rates observed from the studied section were not consistent with this plausible prediction. In contrast, three abrupt changes (~4.6, 3.6, and 2.1 Ma) were detected through the high-resolution magnetostratigraphic data (Figure 10). More likely, the basinward propagation of the provenances was induced by the pulsating exhumation of the ranges. Moreover, the deceleration of dextral slip between Pamir and Tarim was accommodated in the Eastwestern Kongur extensional system (Figure 11) (Arnaud et al., 1993; Brunel et al., 1994; Robinson et al., 2004; Sobel et al., 2011). Plentiful detrital zircons ages are synchronous with major fluvial sedimentation phases, at the outlets of the northeast-flowing rivers in the Tarim Basin, suggesting rapid Pliocene–Quaternary exhumation of the extensional system (Cao et al., 2013; Cao et al., 2018).

Constraints on the tectonic-sedimentary process during the Pliocene

The pre-Pliocene deposits of the Western Kunlun Mountain front record the transition in the depositional environment from the shallow marine to the inland sea, then to a foreland basin in response the to northward impact of the Pamir salient on the basin (Zhang et al., 2001; Bosboom et al., 2011; Sun and Jiang., 2013; Bosboom et al., 2014; Li et al., 2017; Li et al., 2019). Since the Pliocene, the Artux Formation and the Xiyu Formation have been deposited along the Western Tarim Basin margins, and have been considered as the molasse in the foreland basin. These upward coarsening successions provide important information on the growth processes of the surrounding ranges (Zheng et al., 2000). In some sections, eolian sandstone was also identified within these coarse sediments, providing crucial evidence for the inland desertification origin (Sun and Liu, 2006; Zheng et al., 2015a; Sun et al., 2015). Thus, the Artux Formation was most closely related to the present geologic environment and the modern river systems (Figure 11).

During the Pliocene, the depositional systems from source to sink might have changed over time, as a result of the northward encroaching and the intense basinward thrusting of the orogenic belts. The strata of the Yengisar section show the shift upwardly from distal to middle fan systems during the depositional periods of the Artux Formation (Supplementary Figure S1). Subsequently, the alluvial fan gradually propagated basinward until the termination of the Xiyu Formation. The seismic section profile indicated that the basal age of the Xiyu conglomerate and the commencement of growth strata occurred in the early Pleistocene (1.9 Ma) and the late Pleistocene (1.45 Ma), respectively (Figure 3). These ages were estimated by the ratio of 1.8, obtained using the ratio of the Artux Formation to the Xiyu Formation sedimentation rate from the Kekeya section (Zheng et al., 2002). The Yengisar anticline showed a fold deformation at approximately 1.45 Ma, corresponding to the depositional

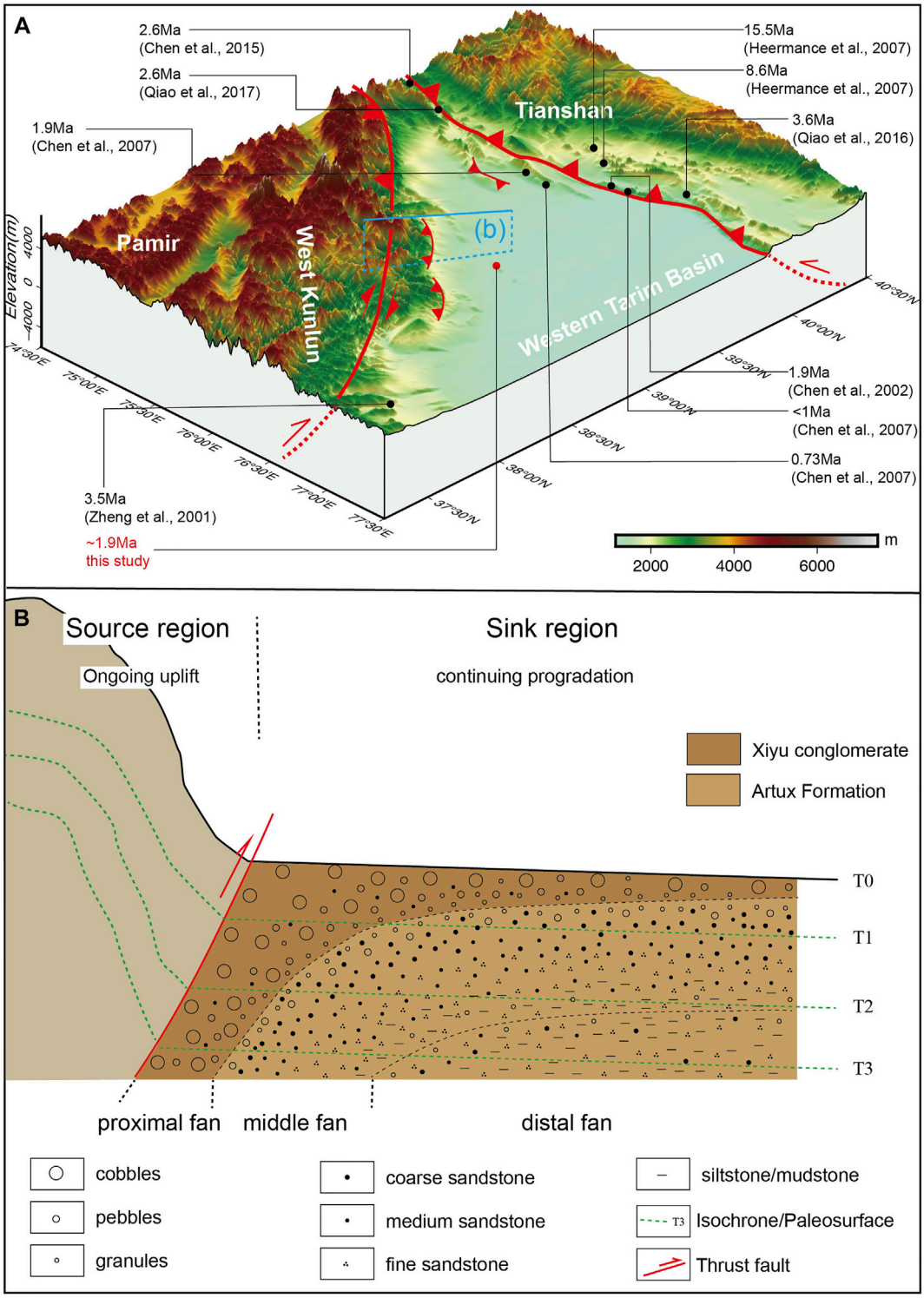

FIGURE 12
(A), Basal ages of the Xiyu Formation in the edge of western Tarim Basin. **(B)**, Conceptual model of the progradational alluvial fan of upward coarsening deposits in the piedmont of an ongoing uplift mountain.

age of the Xiyu Formation (Pan et al., 2009; Fu et al., 2010; Li et al., 2010; Liu et al., 2011).

New perspective on progradation of the Artux Formation and Xiyu Formation

Based on detailed magnetostratigraphy of the upper Cenozoic strata from seven sections in the Southwestern Tian Shan, Chen et al. (2007a) suggested that the basal age of the Xiyu Formation ranges from 15.5 Ma at the northernmost part of the foreland, to 8.6 Ma in the central part of the foreland (Heermance et al., 2007), and from 1.9 Ma, to 0.73 Ma along the southern deformation front of the foreland basin (Figure 12A).

Recently, Qiao et al. (2016) published a new magnetostratigraphic data of the Neogene successions in Kashi area and suggested that the basal age of the Xiyu Formation is 3.6 Ma. On the other hand, in the northeastern part of the West Kunlun Mountain, detailed magnetostratigraphy of 4.5 km Kekeya section near Yecheng showed that the onset of the Xiyu Formation was commenced at 3.5 Ma (updated to ~15 Ma by new chronological data, with refutation) (Zheng et al., 2000, 2015a, 2015b; Sun et al., 2015), whereas the age of the basal conglomerate in the Yengisar section is ~1.9 Ma in this study. All these data suggest that the Xiyu Formation is highly time-transgressive and cannot be considered a chronostratigraphic rock unit (Chen et al., 2007b; Heermance et al., 2007; Qiao et al., 2016).

There are two competing hypotheses of the sedimentary transition recorded in the Xiyu Formation. The first emphasizes that the increases in grain sizes of sediments were caused by frequent and abrupt climate changes during the post-Late Pliocene (Molnar et al., 1993; Zhang et al., 2001; Wang et al., 2003). While another hypothesis argues that the massive conglomerates are the sedimentary response of an intense exhumation of the orogeny related to continuous India-Eurasia convergence (Huang, 1957; Li et al., 1979; Zheng et al., 2000; Chen et al., 2001; Huang et al., 2006; Zhao., 2019).

The conformable contact showed the lack of significant tectonic movement when the Artux Formation deposition translated to the Xiyu Formation in some outcrops. This is one of the main pieces of evidence for advocates of climate hypotheses to disapprove tectonic-driven theory (Zhang, 2004; Zhao et al., 2008b). However, from the source-to-sink perspective, the conformable contact showed that the tectonic environment in the sink region was relatively equable. The abrupt increase in sediment particle size in the sink region is due to the strong uplift in the source region (Figure 12B). In fact, the initial depositional age of the Xiyu Formation ranges from 15.5 Ma to less than 1 Ma, which does not reconcile the climate origin models, due to the synchronous climate changes.

It seems reasonable that the spatiotemporal variation in tectonic uplift events explains the time-transgressive of the massive conglomerates. However, explaining the diachronous successions in the local area (southwestern piedmont of the Tian Shan) remains unclear. Indeed, Chen et al. (2007a) proposed the progradation model to address this issue. They argued that the extension of the thrust fold belt toward the interior of the basin was well consistent with the basal age changes of the conglomerate, thus, the propagation of the conglomerate is directly controlled by local tectonic deformation. Is there a straightforward causal linkage between basinward progradation of conglomerate and pulsed migration of deformation?

Certainly, the increase in gravel progradation rates appears linked to higher deformation rates across the piedmont anticlines in the Southwestern Tian Shan since 5 Ma (Chen et al., 2007b; Heermance et al., 2007). There is no consensus on the sequential onset between the bottom of the Xiyu Formation and the growth strata that represent tectonic deformation in the piedmont of the Southwestern Tian Shan and the northeastern part of West Kunlun Mountain (Figures 1, 2). Unlike the Southwestern Tian Shan, in front of the West Kunlun Mountain, the growth strata in the Kekeya section were developed mainly in the Artux Formation (Zheng et al., 2002). Therefore, no causal links exist between the diachrony of the Xiyu Formation and the migration of the local tectonic deformations.

We put forward a new perspective that both the conglomerate progradation and migration of the deformation front are the sink region responses to the uplift events of the source region, in sedimentology and structural geology, respectively.

The Artux Formation and the Xiyu Formation were originally considered to be a suite of typical molasse deposits. According to Zheng et al. (2002), Chen et al. (2007a), Zhao, (2019), the Artux Formation is typical in braided river facies, and some depositional segments are mid-fan to distal fan sub-facies, filled in an alluvial-fan system draining from the West in the Kashi subbasin (Wei et al., 2013). On the other hand, the lower part of the Xiyu Formation comprises middle and distal alluvial fan facies, while and the upper part is mainly proximal fan sub-facies (Figure 12B). Indeed, facies analysis showed that both formations are typical progradation alluvial fan models. At a fixed fan cross-section, the sediments coarsen upwards over time due to the onset of the orogenic front. The progressive migration of the alluvial fan basinward resulted from the uplift events of the orogen. The development of the prograding alluvial fan strata is different from that of the interior of a large-scale stable basin. In the former conditions, its stratigraphic layers have an obvious time-transgressive feature (Figure 12).

On the other hand, induced by the incremental altitude difference, the lateral extrusion gradually propagates from the bottom of the mountain to the basin, accompanied by the immense uplift.

Based on the results of remote sensing techniques, field investigations, tectonic geomorphology as well as active tectonic in the edge of Southwestern Tarim Basin, reported by several researchers (Pan et al., 2009; Fu et al., 2010; Li et al., 2010; Liu et al., 2011), the frontal thrust belt of the mountains are attributed to the boundary fault of the plateau in the form of thrusting extension in Pliocene and Pleistocene (Qu et al., 2005). In other words, the syntectonic growth strata have deposited on the flanks of one anticline during the tectonic deformation stage, which belongs to the structural geologic response to the continuous uplift of the surrounding mountains.

Conclusion

In this study, a detailed magnetostratigraphic investigation in the Yengisar section located at the southwestern part of the Tarim Basin was conducted. This investigation provided a high-resolution chronology for the Pliocene sedimentary successions. In fact, magnetic polarity zones correlation suggests that the sampled successions were deposited from the ~4.9 Ma to 1.9 Ma. Combining the seismic reflection profile and previous magnetostratigraphic data in this region, the Xiyu Formation and the growth strata began deposited at about 1.9 and 1.45 Ma, respectively.

On the other hand, the observed sedimentation rate revealed a gradual decrease, from >30.9 cm/kyr at 4.9 Ma to 2.9 cm/kyr at 4.6 Ma. This 10-times decrease in sedimentation rate was induced by the weakening of the topographic uplift of the Western Kunlun Mountain. In addition, abrupt increases were found in the sedimentation rate, from ~8 to ~19 cm/kyr at 3.6 Ma and from ~19 cm/kyr to >62.3 cm/kyr at 2.1 Ma. These increases in sedimentation rate are due to the propagations of the strong basinward thrusting triggered by the pulsating growth of the Western Kunlun Mountain.

The basal age of the Xiyu Formation varies from Middle Miocene to Late Pleistocene. Diachrony of the Late Cenozoic upward-coarsening deposits is the result of the alluvial fan propagation induced by continued uplift and increased exhumation of the mountains. We favor the tectonic-theory for the origin of massive conglomerate and argue that the time-transgressive of the basal layer is an intrinsic feature of alluvial fan propagation rather than the migration of the local deformation front.

Data availability statement

The datasets presented in this study can be found in online repositories. The names of the repository/repositories and accession number(s) can be found below: https://github.com/zifeizzz/Data_PMD.

Author contributions

ZZ: Conceptualization, methodology, investigation, formal analysis, writing—original draft; JP: Conceptualization, funding acquisition, resources, supervision, writing—review, and editing; JL: Resources, investigation, review, and editing; YC: Investigation, data preparation, review, and editing; LH: Investigation, visualization, review, and editing.

Funding

This work was financially supported by the Second Tibetan Plateau Scientific Expedition and Research Program (STEP) (2019QZKK0901), the National Natural Science Foundation of China (Grant 42002243, 41672202).

Acknowledgments

We thank the Editor and reviewers for providing constructive comments and suggestions leading to the improvement of the manuscript.

Conflict of interest

The authors declare that the research was conducted in the absence of any commercial or financial relationships that could be construed as a potential conflict of interest.

Publisher's note

Supplementary material

The Supplementary Material for this article can be found online at: https://www.frontiersin.org/articles/10.3389/feart.2022.967346/full#supplementary-material

SUPPLEMENTARY FIGURE S1
Detailed stratigraphic level for sampling.

References

Arnaud, N. O., Brunel, M., Cantagrel, J. M., and Tapponnier, P. (1993). High cooling and denudation rates at Kongur Shan, Eastern Pamir (Xinjiang, China) revealed by40Ar/39Ar alkali feldspar thermochronology. *Tectonics* 12 (6), 1335–1346. doi:10.1029/93tc00767

BGMRXJ (Bureau of Geology and Mineral Resources of Xingjiang Uygur Autonomous Region) (1999). *Rocks and strata of Xinjiang Uygur Autonomous Region*. Wuhan: China University of Geosciences Press (in Chinese)

Borradaile, G. J., and Henry, B. (1997). Tectonic applications of magnetic susceptibility and its anisotropy. *Earth-Science Rev.* 42 (1-2), 49–93. doi:10.1016/s0012-8252(96)00044-x

Borradaile, G. J., and Jackson, M. (2004). Anisotropy of magnetic susceptibility (AMS): Magnetic petrofabrics of deformed rocks. *Geol. Soc. Lond. Spec. Publ.* 238 (1), 299–360. doi:10.1144/gsl.sp.2004.238.01.18

Bosboom, R., Dupont-Nivet, G., Grothe, A., Brinkhuis, H., Villa, G., Mandic, O., et al. (2014). Timing, cause and impact of the late Eocene stepwise sea retreat from the Tarim Basin (west China). *Palaeogeogr. Palaeoclimatol. Palaeoecol.* 403, 101–118. doi:10.1016/j.palaeo.2014.03.035

Bosboom, R. E., Dupont-Nivet, G., Houben, A. J. P., Brinkhuis, H., Villa, G., Mandic, O., et al. (2011). Late Eocene sea retreat from the Tarim Basin (west China) and concomitant Asian paleoenvironmental change. *Palaeogeogr. Palaeoclimatol. Palaeoecol.* 299 (3-4), 385–398. doi:10.1016/j.palaeo.2010.11.019

Brunel, M., Arnaud, N., Tapponnier, P., Pan, Y., and Wang, Y. (1994). Kongur Shan normal fault: Type example of mountain building assisted by extension (Karakoram fault, eastern Pamir). *Geol.* 22 (8), 707. doi:10.1130/0091-7613(1994)022<0707:Ksnfte>2.3.Co;2

Burtman, V., S., and Molnar, P., (1993). Geological society of America special papers] geological and geophysical evidence for deep subduction of continental crust beneath the Pamir volume 281 || *Geol. Geophys. Evid. Deep Subduction Cont. Crust Beneath Pamir*. doi:10.1130/SPE2811–76

Cao, K., Bernet, M., Wang, G.-C., van der Beek, P., Wang, A., Zhang, K.-X., et al. (2013). Focused pliocene–quaternary exhumation of the eastern Pamir domes, Western China. *Earth Planet. Sci. Lett.* 363, 16–26. doi:10.1016/j.epsl.2012.12.023

Cao, K., Mai, H., Wang, G., and Zhang, K. (2018). Mesozoic-Cenozoic tectonic and topographic development of the Pamir syntaxis and its potential effects on the sea retreat in the Tarim Basin. *Quat. Sci.* 38 (1), 15–38. (in Chinese with English abstract). doi:10.11928/j.issn.1001-7410.2018.01.02

Charreau, J., Gilder, S., Chen, Y., Dominguez, S., Avouac, J.-P., Sen, S., et al. (2006). Magnetostratigraphy of the yaha section, Tarim Basin (China): 11 Ma acceleration in erosion and uplift of the tian Shan mountains. *Geol.* 34 (3), 181. doi:10.1130/g22106.1

Charreau, J., Gumiaux, C., Avouac, J. P., Augier, R., Chen, Y., Barrier, L., et al. (2009). The Neogene Xiyu Formation, a diachronous prograding gravel wedge at front of the Tianshan: Climatic and tectonic implications. *Earth Planet. Sci. Lett.* 287, 298–310. doi:10.1016/j.epsl.2009.07.035

Chen, H., Chen, S., and Lin, X. (2014). A Review of the cenozoic tectonic evolution of Pamir syntax. *Adv. Earth Sci.* 29 (8), 890–902. (in Chinese with English abstract). doi:10.11867/j.issn.1001-8166.2014.08.0890

Chen, J., Burbank, D. W., Scharer, K. M., Sobel, E., Yin, J., Rubin, C., et al. (2002). Magnetochronology of the upper cenozoic strata in the southwestern Chinese tian Shan: Rates of Pleistocene folding and thrusting. *Earth Planet. Sci. Lett.* 195 (1-2), 113–130. doi:10.1016/s0012-821x(01)00579-9

Chen, J., Heermance, R., Burbank, D. W., Scharer, K. M., Miao, J., Wang, C., et al. (2007a). Quantification of growth and lateral propagation of the Kashi anticline, southwest Chinese Tian Shan. *J. Geophys. Res.* 112 (B3), B03S16. doi:10.1029/2006jb004345

Chen, J., Heermance, R. V., Burbank, D. W., Scharer, K. M., and Wang, C. (2007b). Magnetochronology and its implications of the Xiyu conglomerate in the southwestern Chinese tian Shan foreland. *Quat. Sci.* 27 (4), 576–587. (in Chinese with English abstract). doi:10.3321/j.issn:1001-7410.2007.04.014

Chen, J., Lu, Y., and Ding, G. (2001). Records of late Cenozoic mountain building in Western Tarim basin:molasses, growth strata and growth unconformity. *Quat. Sci.*, 528–539. (in Chinese with English abstract). doi:10.1360/zd-2013-43-7-1168

Chen, J., Yi, J., Qu, G. S., and Zhang, K. (2000). Timing, lower boundary, Genesis, and deformation of Xiyu formation around the Western margins of the Tarim basin. *Seismol. Geol.* 22 (S), 104–116. (in Chinese with English abstract). doi:10.1360/zd-2013-43-7-1168

Chen, X., Chen, H., Cheng, X., Shen, Z., and Lin, X. (2015). Sedimentology and magnetostratigraphy of the tierekesazi cenozoic section in the foreland region of south west tian Shan in western China. *Tectonophysics* 654, 156–172. doi:10.1016/j.tecto.2015.05.009

Cowgill, E. (2010). Cenozoic right-slip faulting along the eastern margin of the Pamir salient, northwestern China. *Geol. Soc. Am. Bull.* 122 (1-2), 145–161. doi:10.1130/b26520.1

Fisher, R. (1953). Dispersion on a sphere. *Proc. R. Soc. A Math. Phys. Eng. Sci.* 217 (1130), 295–305. doi:10.1098/rspa.1953.0064

Fu, B., Ninomiya, Y., and Guo, J. (2010). Slip partitioning in the northeast Pamir–Tian Shan convergence zone. *Tectonophysics* 483 (3-4), 344–364. doi:10.1016/j.tecto.2009.11.003

Gao, M. (2012). *Geometry and kinematics of the western part of Southwest Tarim Basin*. Beijing), Beijing: China University of Geosciences.

Gradstein, F. M., Ogg, J. G., and Hilgen, F. J. (2012). On the geologic time scale. *Newsl. Stratigr.* 45 (2), 171–188. doi:10.1127/0078-0421/2012/0020

Guo, X., Ding, X., and He, X. (2002). New progress in the study of marine transgressional events and marine strata of the meso-cenozoic in the Tarim Basin. *Acta Geol. Sin.* 76 (3), 299–307. (in Chinese with English abstract). doi:10.3321/j.issn:0001-5717.2002.03.002

Harrison, R. J., Muraszko, J., Heslop, D., Lascu, I., Muxworthy, A. R., Roberts, A. P., et al. (2018). An improved algorithm for unmixing first-order reversal curve diagrams using principal component analysis. *Geochem. Geophys. Geosyst.* 19 (5), 1595–1610. doi:10.1029/2018gc007511

Heermance, R. V., Chen, J., Burbank, D. W., and Wang, C. (2007). Chronology and tectonic controls of Late Tertiary deposition in the southwestern Tian Shan foreland, NW China. *Basin Res.* 19 (4), 599–632. doi:10.1111/j.1365-2117.2007.00339.x

Huang, B., Piper, J., Peng, S., Liu, T., Li, Z., Wang, Q., et al. (2006). Magnetostratigraphic study of the kuche depression, Tarim Basin, and cenozoic uplift of the tian Shan range, western China. *Earth Planet. Sci. Lett.* 251 (3-4), 346–364. doi:10.1016/j.epsl.2006.09.020

Huang, J., 1957. Several types of neotectonics in China. In: (Editor), *The first speech of Chinese Academy of Sciences about neotectonic movement*. Science Press, Beijing, pp. 44.C.A.o.S. Division of Earth Sciences

Kirschvink, J. L. (1980). The least-squares line and plane and the analysis of palaeomagnetic data. *Geophys. J. Int.* 62 (3), 699–718. doi:10.1111/j.1365-246x.1980.tb02601.x

Koymans, M. R., Hinsbergen, D. J. J., Pastor-Galán, D., Vaes, B., and Langereis, C. G. (2020). Towards FAIR paleomagnetic data management through Paleomagnetism.org 2.0. *Geochem. Geophys. Geosyst.* 21 (2), e2019GC008838. doi:10.1029/2019gc008838

Li, D., Zhao, Y., Liu, J., Pan, Y., and He, Z. (2010). Late cenozoic tectonic deformation on the northwestern margin of the qinghai-tibet plateau. *Acta Geol. Sin.* 84 (03), 293–310. (in Chinese with English abstract).

Li, J., Tongwen, W. U., and Lei, Y. (2019). Geology and geomorphology of Tarim Basin and its evolution in the cenozoic. *Geol. J. China Univ.* 25 (3), 466–473. (in Chinese with English abstract). doi:10.16108/j.issn1006-7493.2018100

Li, J., Wen, S., Zhang, Q., Wang, F., Zhen, B., and Li, B. (1979). Age, magnitude and manner of the uplift of the Qinghai-Tibet Plateau. *Sci. China* 6, 608–616. (in Chinese).

Li, J., Zhao, Y., Pei, J. L., Liu, F., Zhou, Z. Z., Gao, H. L., et al. (2017). Cenozoic marine sedimentation problem of the Tarim basin. *J. Geomechanics* 23 (01), 141–149. (in Chinese with English abstract). doi:10.3969/j.issn.1006-6616.2017.01.010

Liu, D., Li, H., Sun, Z., Cao, Y., Wang, L., Pan, J., et al. (2017). Cenozoic episodic uplift and kinematic evolution between the Pamir and Southwestern Tien Shan. *Tectonophysics* 712-713, 438–454. doi:10.1016/j.tecto.2017.06.009

Liu, D. L., Li, H. B., Pan, J. W., Chevalier, M. L., and Pei, J. L. (2011). Morphotectonic study from the northeastern margin of the Pamir to the West Kunlun range and its tectonic implications. *Acta Petrol. Sin.* 27 (11), 3499–3512. (in Chinese with English abstract).

Métivier, F., and Gaudemer, Y. (1997). Mass transfer between eastern tien Shan and adjacent basins (central asia): Constraints on regional tectonics and topography. *Geophys. J. Int.* 128 (1), 1–17. doi:10.1111/j.1365-246X.1997.tb04068.x

Molnar, P., and England, P. (1990). Late cenozoic uplift of mountain ranges and global climate change: Chicken or egg? *Nature* 346 (6279), 29–34. doi:10.1038/346029a0

Molnar, P., England, P., and Martinod, J. (1993). Mantle dynamics, uplift of the Tibetan plateau, and the Indian monsoon. *Rev. Geophys.* 31 (4), 357. doi:10.1029/93rg02030

Pan, J., Li, H., Vander, W., Sun, Z., Pei, J., Si, J., et al. (2009). Tectonic geomorphology and active tectonics in northeastern Pamir, northwest margin of Qinghai-Tibet plateau. *Quat. Sci.* 29 (03), 586–598. (in Chinese with English abstract). doi:10.3969/j.issn.1001-7410.2009.03.19

Pei, J., Li, H., Sun, Z., Si, J., and Ren, X. (2011a). Constraints the uplift age of maza tagh mountain in the centre of tarim basin and its climatic implications. *Acta Petrol. Sin.* 27 (1), 333–343. (in Chinese with English abstract).

Pei, J. L., Li, H. B., Si, J. L., Pan, J. W., and Zhao, Y. (2011b). The response of the Tibet uplift since Lower Pleistocene in the centre of Tarim basin. *Acta Petrol. Sin.* 27 (11), 3487–3498. (in Chinese with English abstract).

Pei, J. L., Sun, Z. M., Li, H. B., Si, J. L., and Zhao, Y. (2008). Paleocurrent direction of the Late Cenozoic sedimentary sequence of the Tibetan plateau Northwestern margin constrained by AMS and its tectonic implications. *Acta Petrol. Sin.* 24 (7), 1613–1620. (in Chinese with English abstract).

Qiao, Q., Huang, B., Biggin, A. J., and Piper, J. D. A. (2017). Late Cenozoic evolution in the Pamir-Tian Shan convergence: New chronological constraints from the magnetostratigraphic record of the southwestern Tianshan foreland basin (Ulugqat area). *Tectonophysics* 717, 51–64. doi:10.1016/j.tecto.2017.07.013

Qiao, Q., Huang, B., Piper, J. D. A., Deng, T., and Liu, C. (2016). Neogene magnetostratigraphy and rock magnetic study of the Kashi depression, NW China: Implications to neotectonics in the SW tianshan mountains. *J. Geophys. Res. Solid Earth* 121 (3), 1280–1296. doi:10.1002/2015jb012687

Qu, G. S., Li, Y. G., and Li, Y. F. (2005). Tectonic segmentation and its origin of southwestern Tarim foreland basin. *Sci. China (Ser. D Earth Sci.* 35 (03), 193–202. (in Chinese with English abstract). doi:10.3969/j.issn.1674-7240.2005.03.001

Qu, G. S., Li, Y. G., and Zhang, N. (2004). A study on the foreland structure of the qimugen arc in southwest tarim and its genetic mechanism. *Geol. Rev.* 50 (6), 567–576. (in Chinese with English abstract). doi:10.3321/j.issn:0371-5736.2004.06.007

Robinson, A. C., Yin, A., Manning, C. E., Harrison, T., Zhang, S., Wang, X.-f., et al. (2004). Tectonic evolution of the northeastern Pamir: Constraints from the northern portion of the Cenozoic Kongur Shan extensional system, Western China. *Geol. Soc. Am. Bull.* 116, 953. doi:10.1130/b25375.1

Sobel, E. R., Schoenbohm, L. M., Chen, J., Thiede, R., Stockli, D. F., Sudo, M., et al. (2011). Late miocene–pliocene deceleration of dextral slip between Pamir and tarim: Implications for Pamir orogenesis. *Earth Planet. Sci. Lett.* 304 (3-4), 369–378. doi:10.1016/j.epsl.2011.02.012

Sun, J., Alloway, B., Fang, X., and Windley, B. F. (2015). Refuting the evidence for an earlier birth of the Taklimakan Desert. *Proc. Natl. Acad. Sci. U. S. A.* 112 (41), E5556–E5557. doi:10.1073/pnas.1517525112

Sun, J., and Jiang, M. (2013). Eocene seawater retreat from the southwest Tarim Basin and implications for early Cenozoic tectonic evolution in the Pamir Plateau. *Tectonophysics* 588, 27–38. doi:10.1016/j.tecto.2012.11.031

Sun, J., and Liu, T. (2006). The age of the taklimakan desert. *Science* 312 (5780), 1621. doi:10.1126/science.1124616

Sun, J., Windley, B. F., Zhang, Z., Fu, B., and Li, S. (2016). Diachronous seawater retreat from the southwestern margin of the Tarim Basin in the late Eocene. *J. Asian Earth Sci.* 116, 222–231. doi:10.1016/j.jseaes.2015.11.020

Tang, Z., Dong, X., Wang, X., and Ding, Z. (2015). Oligocene-Miocene magnetostratigraphy and magnetic anisotropy of the Baxbulak section from the Pamir-Tian Shan convergence zone. *Geochem. Geophys. Geosyst.* 16 (10), 3575–3592. doi:10.1002/2015gc005965

Tarling, D., and Hrouda, F. (1993). *Magnetic anisotropy of rocks*, XII. London: Chapman & Hall, 218.

Tauxe, L., Mullender, T. A. T., and Pick, T. (1996). Potbellies, wasp-waists, and superparamagnetism in magnetic hysteresis. *J. Geophys. Res.* 101 (B1), 571–583. doi:10.1029/95jb03041

Wang, E., Wan, J., and Liu, J. (2003). Late Cenozoic geological evolution of the foreland basin bordering the West Kunlun range in Pulu area: Constraints on timing of uplift of northern margin of the Tibetan Plateau. *J. Geophys. Res.* 108 (B8), 2401. doi:10.1029/2002jb001877

Wei, H.-H., Meng, Q.-R., Ding, L., and Li, Z.-Y. (2013). Tertiary evolution of the Western Tarim Basin, northwest China: A tectono-sedimentary response to northward indentation of the Pamir salient. *Tectonics* 32 (3), 558–575. doi:10.1002/tect.20046

Westerhold, T., Marwan, N., Drury, A. J., Liebrand, D., Agnini, C., Anagnostou, E., et al. (2020). An astronomically dated record of Earth's climate and its predictability over the last 66 million years. *Science* 369 (6509), 1383–1387. doi:10.1126/science.aba6853

Xu, Z. Q., Li, S. T., Zhang, J. X., Yang, J. S., and Cai, Z. H. (2011). Paleo-Asian and Tethyan tectonic systems with docking the Tarim block. *Acta Petrol. Sin.* 27 (1), 1–22. (in Chinese with English abstract).

Yang, W., Dupont-Nivet, G., Jolivet, M., Guo, Z., Bougeois, L., Bosboom, R., et al. (2015). Magnetostratigraphic record of the early evolution of the southwestern Tian Shan foreland basin (Ulugqat area), interactions with Pamir indentation and India–Asia collision. *Tectonophysics* 644-645, 122–137. doi:10.1016/j.tecto.2015.01.003

Zhang, P. (2004). Late Cenozoic tectonic deformation in the Tianshan Mountain and its foreland basins. *Chin. Sci. Bull.* 49 (4), 311. doi:10.1360/03wd0488

Zhang, P., Molnar, P., and Downs, W. R. (2001). Increased sedimentation rates and grain sizes 2-4 Myr ago due to the influence of climate change on erosion rates. *Nature* 410 (6831), 891–897. doi:10.1038/35073504

Zhao, Y., Li, D., Liu, J., Pan, Y., He, Z., Xu, G., et al. (2008a). Xiyu conglomerate and structural deformation of northwestern margin of Tibetan Plateau. *Bull. Mineralogy, Petrology Geochem.* 27 (S1), 415. doi:10.3969/j.issn.1007-2802.2008.z1.222

Zhao, Y., Li, D. P., Liu, J., Wang, Y., and Zhang, S. H. (2008b). Tectonic geomorphology: A key to understanding of the history of the plateau. *Geol. Bull. China* 28 (12), 1961–1967. (in Chinese with English abstract). doi:10.3969/j.issn.1671-2552.2008.12.002

Zhao, Y. (2019). *The sedimentary characteristics and tectonic significance of Xiyu conglomerate of late Pliocene to early Pleistocene in northeastern Pamir, Xinjiang*. Beijing: Chinese Academy of Geological Sciences.

Zheng, H. B., Butcher, K., and Powell, C. (2002). Evolution of Neogene foreland basin in Yecheng, Xinjiang, and uplift of northern Tibetan plateau——I stratigraphy and petrology. *Acta Sedimentol. Sin.* 20 (02), 274–281. (in Chinese with English abstract). doi:10.3969/j.issn.1000-0550.2002.02.015

Zheng, H. B., Butcher, K., and Powell, C. (2003). Evolution of Neogene foreland basin in Yecheng, Xinjiang, and uplift of northern Tibetan plateau——II facies analysis. *Acta Sedimentol. Sin.* 21 (01), 46–51. (in Chinese with English abstract). doi:10.3969/j.issn.1000-0550.2003.01.008

Zheng, H., Powell, C. M., An, Z., Zhou, J., and Dong, G. (2000). Pliocene uplift of the northern Tibetan Plateau. *Geol.* 28 (8), 715. doi:10.1130/0091-7613(2000)28<715:Puotnt>2.0.Co;2

Zheng, H., Wei, X., Tada, R., Clift, P. D., Wang, B., Jourdan, F., et al. (2015a). Late oligocene-early Miocene birth of the taklimakan desert. *Proc. Natl. Acad. Sci. U. S. A.* 112 (25), 7662–7667. doi:10.1073/pnas.1424487112

Zheng, H., Wei, X., Tada, R., Clift, P. D., Wang, B., Jourdan, F., et al. (2015b). Reply to Sun et al.: Confirming the evidence for Late Oligocene–Early Miocene birth of the Taklimakan Desert. *Proc. Natl. Acad. Sci. U. S. A.* 112 (41), E5558–E5559. doi:10.1073/pnas.1517735112

Zhou, Z. Z., Pei, J. L., Feng, L. J., Liu, F., Sheng, M., and Zhao, Y. (2016). New evidence for rotation of northeastern Pamir since late cenozoic. *Chin. J. Geophys.* 59 (02), 633–642. (in Chinese with English abstract). doi:10.6038/cjg20160220